Thermal Decomposition of Energetic Materials. 25. Shifting of the Dominant Decomposition Site by Backbone Substitution of Alkylammonium Nitrate Salts

Y. Oyumi and T. B. Brill*

Department of Chemistry, University of Delaware, Newark, Delaware 19716 *(Received: December 1, 1986)*

Exchanging X = $-C(NO_2)_2F$ for X = $-C(NO_2)_3$ causes the dominating fast thermal decomposition site in $[X-CH_2CH_2NH_3]NO_3$ salts to shift from largely that of the C–NO_2 bond to largely that of the $-H^+\cdots NO_3^-$ portion. This is consistent with an order of thermal stability of the energetic sites in these salts of $-C(NO_2)_2F > -H^+\cdots NO_3^- > -C(NO_2)_3$. These conclusions were drawn from the nature of the IR-active gas products that are evolved in real time upon fast thermolysis (>100 K s^{-1}) and from slow heating of the condensed phase. The O/H ratio of the parent primary ammonium salt appears to be a qualitative indicator of whether NH_3(g) will be formed under these conditions. Salts with O/H ≥ 1 have not been observed to release NH_3(g) while those with O/H < 1 do. The salt with X = $-C(NO_2)_2F$ possesses four polymorphs between 297 K and its two melting points. Only two polymorphs are present when X = $-C(NO_2)_3$.

Introduction

An aspect of the thermal decomposition of energetic materials in the condensed phase that has interested us is the situation in which more than one type of energy-rich site exists in the molecule. One might call these binary energetic molecules.

An example of a binary energetic molecule is in the nitro-nitrosamine (I). By rapid-scan infrared spectroscopy, under rapid

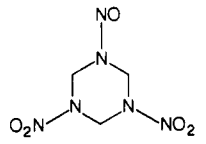

I

thermolysis conditions (>100 K s^{-1}), we detected evidence that reactions involving the nitramine groups of I dominate the thermal decomposition.[1] Likewise, DNFP (II), which contains both

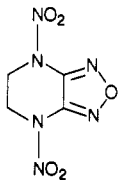

II

nitramine and furazan units, gives evidence that the nitramine units trigger the decomposition.[2] On the other hand, studies of the two other binary energetic molecules, AZTC (III)[3] and DATH (IV),[4] that contain both azidomethyl and nitramine groups suggest

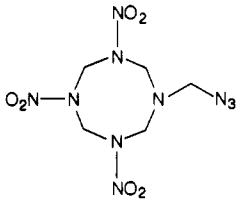

III

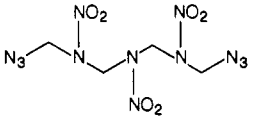

IV

that the azidomethyl group triggers the degradation of the molecule. The thermolysis of TNENG (V), which contains the trinitromethyl unit and a nitrimine group, appears to be triggered by the trinitromethyl group.[5] Thus, without first building an experimental basis, it is not intuitively evident which energetic functional unit is the weaker link during thermolysis.

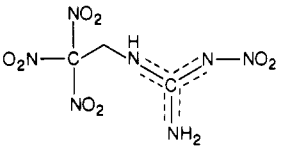

V

Attention in this paper is directed toward comparing the thermolysis products of two nitrate salts, one of which contains the trinitromethyl group, TNPAN (VI), and the other the fluorodinitromethyl entity, FDNPAN (VII). FDNPAN and

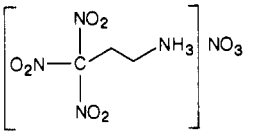

VI

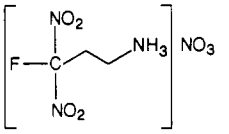

VII

TNPAN provide the opportunity to compare the thermal stability of two related energetic cations containing a common $-H^+\cdots NO_3^-$ group. The relative thermal stabilities of the energetic units can be ascertained. In the course of these studies, extensive polymorphism was also discovered. The polymorphic schemes were characterized by IR spectroscopy and differential thermal analysis.

Experimental Section

Samples of TNPAN and FDNPAN were provided by Dr. H. G. Adolph of NSWC, White Oak, MD. DTA measurements were made on a Mettler 2000B analyzer loaned to us by Dr. M. K. Jain. TGA measurements were made on a DuPont 910 analyzer. For both methods of thermal analysis, dT/dt = 5 K min^{-1}. A flowing He atmosphere was used for TGA, and a static N_2 atmosphere was used for DTA. E_a of decomposition was calculated from the TGA data by the method of Toop[6] and Broid.[7]

All infrared measurements were made on a Nicolet 60SX FTIR spectrometer. Spectra of the solid phase were recorded by transmission IR spectroscopy through a thin film of the sample on an NaCl plate. The film was prepared by evaporating an acetonitrile solution of the sample. The sample was then heated and cooled as desired at a rate of 5 K min^{-1}. Thirty-two spectra at 2-cm^{-1} resoltuion were added to obtain the plots shown in this paper.

High-rate thermolysis studies were conducted using a cell and procedures previously discussed.[8] One milligram of sample was

(1) Oyumi, Y.; Brill, T. B. *Combust. Flame* **1985**, *62*, 233.
(2) Oyumi, Y.; Rheingold, A. L.; Brill, T. B. *J. Phys. Chem.* **1986**, *90*, 4686.
(3) Brill, T. B.; Karpowicz, R. J.; Haller, T. B.; Rheingold, A. L. *J. Phys. Chem.* **1984**, *88*, 4138.
(4) Oyumi, Y.; Rheingold, A. L.; Brill, T. B. *J. Phys. Chem.* **1987**, *91*, 920.
(5) Oyumi, Y.; Brill, T. B. *Propellants, Explos., Pyrotech.*, in press.
(6) Toop, D. J. *IEEE Trans. Electr. Insul.* **1972**, *EI-7*, 1.
(7) Broid, A. *J. Polym. Sci.* **1969**, *H-2*, 7.

0022-3654/87/2091-3657$01.50/0

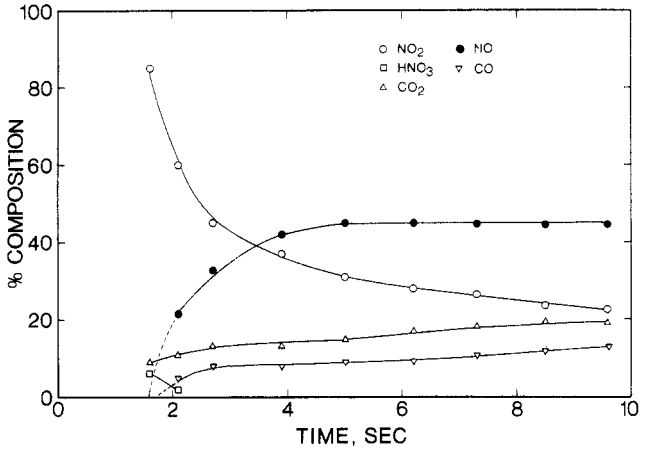

Figure 1. Time dependence of the relative concentrations of the gas products (excluding H_2O and IR-inactive products) from thermolysis of TNPAN at dT/dt = 110 K s^{-1} under 15 psi of Ar. The sample is heating from room temperature to the decomposition temperature range in the initial 1.5 s.

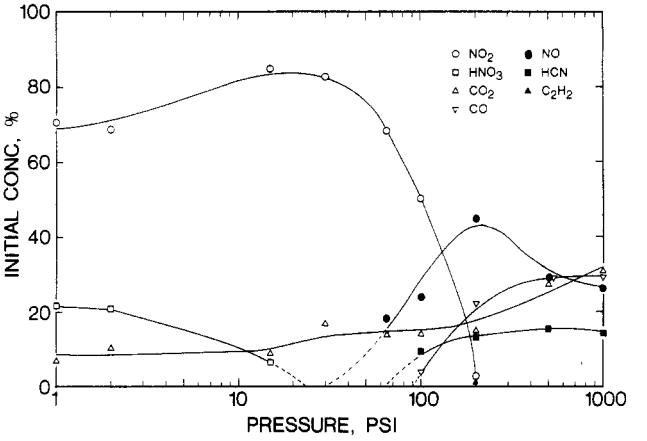

Figure 2. Relative concentrations of the first detected gas products upon thermolysis of TNPAN at dT/dt = 110 K s^{-1} as a function of the static Ar pressure in the cell. H_2O and IR-inactive species are not included. The lines are drawn to connect the points.

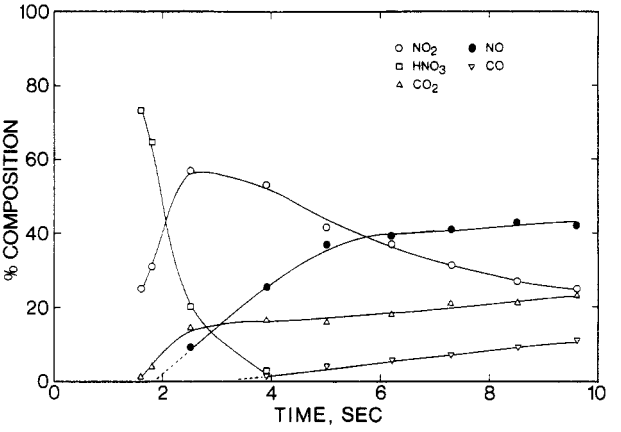

Figure 3. Time dependence of the relative concentrations of the gas products (excluding H_2O and IR-inactive products) from the thermolysis of FDNPAN at dT/dt = 110 K s^{-1} under 15 psi of Ar. The sample is heating from room temperature to the decomposition temperature range in the initial 1.5 s.

spread on a nichrome ribbon filament. The pressure of Ar in the cell was adjusted as desired. The sample was ramp-heated for 3–5 s at the desired rate until a final filament temperature was reached. In the initial 1–2 s no products were detected because the sample is merely heating to its decomposition temperature. Once reached, the filament temperature was then held so that the total duration of heating was 10 s. The IR spectrum of the gas products 2 mm above the surface of the filament was recorded in real time during the 10 s of heating. The scan rate was 10 scans s^{-1} with two spectra per file at 4-cm^{-1} resolution. Using the absolute intensities of characteristic absorptions, we determined the relative concentrations of the IR-active gas products, excluding H_2O and sublimate. The effect of pressure on the product distribution was established by calibrating the filament so that the sample heating rate was about 110 K s^{-1} at each pressure. A separate thermolysis experiment was then performed at each static Ar pressure, and the first observed products were quantified. These concentrations were then plotted vs. pressure to ascertain the role that pressure plays in determining the products initially observed in the gas phase.

Thermal Decomposition

Thermolysis studies of the type described in this paper might seem to be readily conducted by using global kinetics measurements from DSC, DTA, or TGA. Despite the useful data that can be obtained, the similarity of E_a values for many of the decomposition reactions makes it difficult to distinguish the contributions of various groups. Also, sublimation can affect the data.

According to TGA measurements, TNPAN when heated at 5 K min^{-1} loses 77% of its weight between 423 and 439 K. The loss of $3NO_2 + HNO_3$ from TNPAN corresponds to 78%. E_a = 42.8 kcal mol^{-1}, which compares to 40.5 kcal mol^{-1} for NH_4NO_3[9] and 43.2 kcal mol^{-1} for $CH_3C(NO_2)_3$.[10] The determination of E_a for the decomposition of FDNPAN was complicated by the fact that weight loss begins at 395 K, which precedes the decomposition temperature by 30 K. This weight loss is due to sublimation, which probably occurs by proton transfer, desorption of the neutrals, and recombination in the gas phase.[11] Thus, the value of E_a of decomposition for FDNPAN is not reliably obtained from TGA measurements. The characterization of the decomposition of TNPAN and FDNPAN by a molecular process, such as is afforded by infrared spectroscopy, is more informative.

The transmission IR spectrum reveals that TNPAN begins to decompose in the solid phase at about 413 K without melting. Vigorous decomposition takes place in the 423–429 K range. All of the vibrational modes are affected, as might be expected from the weight loss measured by TGA. The same method applied to FDNPAN shows that the decomposition occurs above 433 K. The higher decomposition temperature of FDNPAN compared to TNPAN is consistent with the trend in the activation energy for decomposition of fluorodinitromethyl- and trinitromethyl-containing compounds.[10] The IR spectrum reveals that the intensity of the NO_3^- modes of FDNPAN diminishes before the C–NO_2 modes are affected. This is tentative evidence, to be supported momentarily, that substitution of F for NO_2 in the $-C(NO_2)_3$ group stabilizes this end of the molecule to the point that the $-H^+\cdots NO_3^-$ portion becomes the predominant thermal weak point.

The above differences in the solid-phase IR spectra of these two compounds are manifested in the order of appearance of products in the gas phase. According to Figure 1 for TNPAN, NO_2, which probably forms via homolysis of the C–NO_2 bond, is the dominant early product. HNO_3(g) from proton transfer and desorption is a relatively minor product. CO, CO_2, and NO grow in concentration with time as [NO_2] and [HNO_3] diminish. This behavior is especially evident in the pressure dependence of the first observed thermolysis products shown in Figure 2. At higher pressure, increasingly more stable products are observed first and probably come from later stage reactions. This is because the residence time of the reactive gases in the vicinity of the condensed phase is longer at higher pressure. Hence, the products that are first detected become increasingly "combustion-like" as

(8) Oyumi, Y.; Brill, T. B. *Combust. Flame* **1985**, *62*, 213.
(9) Robertson, A. J. B. *J. Soc. Chem. Ind., London* **1948**, *67*, 221.
(10) Nazin, G. M.; Manelis, G. B. *Izv. Akad. Nauk SSSR, Ser. Khim.* **1972**, 811.
(11) Bircumshaw, L. L.; Newman, B. H. *Proc. R. Soc. London, Ser. A* **1955**, *227*, 228.

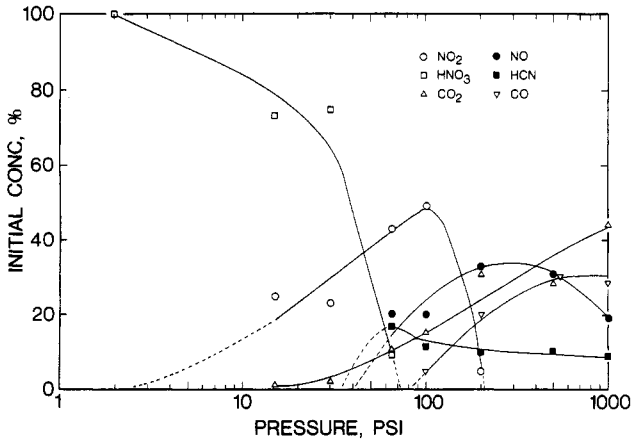

Figure 4. Relative concentrations of the gas products that are first detected during thermolysis of FDNPAN at dT/dt = 110 K s^{-1} as a function of the static Ar pressure in the cell. H_2O and IR-inactive species are not quantified.

the pressure is raised.[12] Curiously, a tiny concentration of C_2H_2 was detected under 200 psi of Ar.

The products of thermolysis of FDNPAN reflect the stabilizing influence of F in place of an NO_2 group. Rather than the dominance of NO_2 from C–NO_2 bond homolysis, Figure 3 reveals that proton transfer leading to HNO_3(g) now is the predominant early reaction. The rise in the NO_2 concentration with time suggests that C–NO_2 bond fission eventually becomes a major reaction but that it lags the proton-transfer step. It is possible that the NO_2 could be formed largely from the decomposition of HNO_3, but in either case, the $-H^+\cdots NO_3^-$ portion of FDNPAN would had to have decomposed before the $F(NO_2)_2C-$ portion. This pattern of relative stability is also supported by the initial concentrations of products as a function of pressure shown in Figure 4. Proton transfer to NO_3^- followed by desorption of HNO_3 is the only detectable reaction at low pressure under these experimental conditions. Since some sublimation is also evident, the evaporation of the neutral amine must have also occurred. NO_2, partly from C–NO_2 bond homolysis and partly from decomposition of HNO_3, is present at intermediate pressures. At still higher pressures, these reactive molecules give way to later stage products characteristic of multistep decomposition reactions because their residence time in and near the condensed phase is longer.

Qualitatively, the presence or absence of NH_3 from fast thermolysis might be expected to depend in part on the oxidizing power of the parent ammonium nitrate salt. A strongly oxidizing environment would not favor the formation of NH_3. NH_3 could form from C–N bond heterolysis of the salt, but it more likely forms from a neutral species following C–N bond homolysis and H• abstraction in the condensed phase. Species arising from H• migration in the heterogeneous gas/condensed phase during fast thermolysis are probably the result of various intra- and intermolecular rearrangements[13] which are difficult to specify. NH_3 is indeed the product of the fast thermolysis of the primary ammonium salts $[C(CH_2NH_3)_4](NO_3)_4$,[14] $[C(NHNH_2)_3]NO_3$,[15] $[NH_3(CH_2)_2NH_3](NO_3)_2$,[16] and NH_4NO_3[15] for which the O/H ratio is less than 1. As the oxidizing power of the parent ammonium nitrate salt becomes larger (here measured by the O/H ratio), $[NH_3]$ might be expected to diminish. This is the case when O/H $\geq$ 1, as it is in $[NH_3OH]NO_3$, where no NH_3 is observed in the gas phase.[17] The presence of NO_2 groups on the aliphatic chain of TNPAN and FDNPAN raises the oxidizing power (O/H $\geq$ 1) to the point that NH_3 does not form. Thus, the O/H ratio qualitatively indicates whether NH_3 will be a product of the fast thermolysis of a primary ammonium nitrate salt.

Similar correlations between the stoichiometry of a parent energetic molecule and the distribution of thermal decomposition products have been reported for nitrate esters[18] and secondary nitramines.[13] These relationships require fast thermolysis, appropriate sample size, and real-time detection, because later stage reactions can interfere. However, they are useful for predicting the probable products from the fast thermal degradation of energetic materials.

In summary, the relative importance of C–NO_2 bond homolysis and the transfer of H^+ to NO_3^- during thermolysis appears to shift as a result of substitution of F for NO_2 in these compounds. The

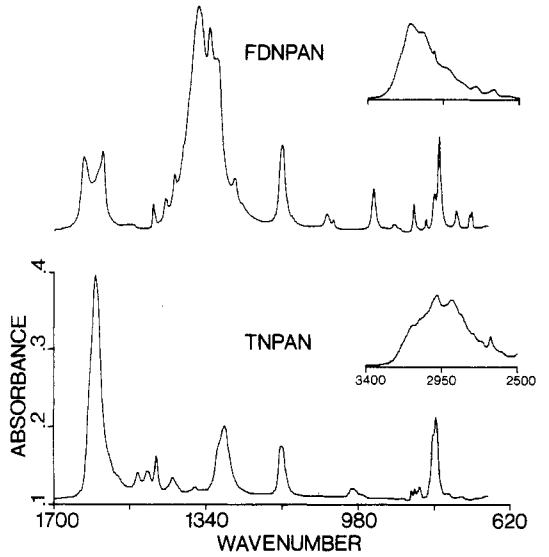

Figure 5. Mid-IR spectra of neat polycrystalline films of FDNPAN and TNPAN at 298 K.

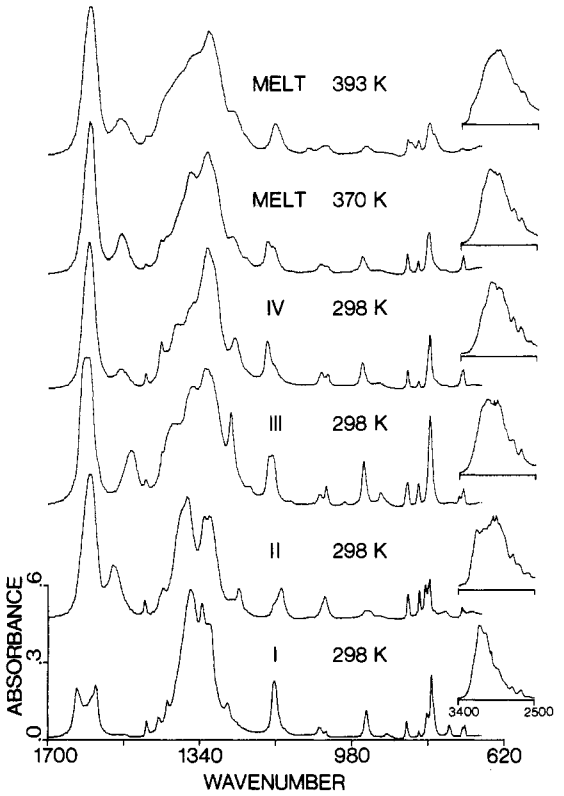

Figure 6. Mid-IR spectra of the polymorphs and melt phases of FDNPAN whose relationship to one another is shown in Figure 7. Solid phases I–IV exhibit hysteresis and can be cooled to 298 K for a brief period of time.

(12) Oyumi, Y.; Brill, T. B. *Combust. Flame*, in press.
(13) Brill, T. B.; Oyumi, Y. *J. Phys. Chem.* **1986**, *90*, 6848.
(14) Oyumi, Y.; Brill, T. B.; Rheingold, A. L.; Lowe-Ma, C. *J. Phys. Chem.* **1985**, *89*, 2309.
(15) Oyumi, Y.; Brill, T. B. *J. Phys. Chem.* **1985**, *89*, 4325.
(16) Russell, T. P.; Brill, T. B., unpublished results.
(17) Cronin, J. T.; Brill, T. B. *J. Phys. Chem.* **1986**, *90*, 178.
(18) Oyumi, Y.; Brill, T. B. *Combust. Flame* **1986**, *66*, 9.

TABLE I: Mid-IR Frequencies (cm^{-1})[a] of FDNPAN Measured on Thin Films of the Pure Material

I (298 K)	II (298 K)	III (298 K)	IV (298 K)	melt (370 K)	melt (393 K)	tent. assignt
3145 m	3187 m	3127 m, sh	3134 m, sh	3133 m, sh	3275 w, sh	$\nu_{as}(NH_3^+)$, $\nu_s(NH_3^+)$
3079 m, sh	3104 m, sh	3059 m		3055 m	3034 m	
	3039 m, sh		3036 m			
3007 m, sh	2991 m	2988 m	2995 m, sh	2993 m	2992 m	$\nu_{as}(CH_2)$, $\nu_s(CH_2)$
2933 w, sh	2954 m	2949 m	2948 m	2949 m	2953 m	
	2918 m, sh	2923 m, sh	2920 m, sh			
	2861 m, sh	2856 m, sh	2865 m, sh	2867 m, sh		
2756 w	2762 w	2771 w	2777 w	2777 w	2764 w	combinations and overtones
2653 w	2696 w	2676 w	2687 w	2687 w	2673 w	
2569 vw	2576 vw	2560 vw	2571 vw	2571 vw		
		2500 vw	2526 vw	2520 vw		
2479 vw	2483 vw	2461 vw	2479 vw	2475 vw		
2438 vw	2414 vw		2430 vw	2416 vw		
2362 vw	2367 vw	2342 vw	2346 vw	2350 vw		
1947 vw, br	2001 vw, br	2013 vw, br	2018 vw, br	2003 vw, br	2011 vw, br	
1758 w	1762 w	1755 w	1757 w	1755 w	1755 w	$(\nu_1 + \nu_4)(NO_3^-)$
1630 m	1601 s	1611 s	1602 s	1600 s	1599 s	$\nu_{as}(NO_2)$, $\delta_{as}(NH_3^+)$
1586 m		1603 s				
1523 vw	1545 m	1502 m	1527 w	1525 m	1527 m	$\delta_s(NH_3^+)$, CH_2 scissor
1466 w	1471 w	1469 w	1469 w	1468 w	1466 w	CH_2 scissor wagging
1437 w	1427 w	1431 m, sh	1432 m	1432 m		
1417 w			1421 m, sh	1418 m, sh	1415 m, sh	
1360 s	1383 s, sh	1401 m	1392 m		1385 m, sh	$\nu_3(NO_3^-)$
	1370 s	1355 s	1366 m, sh	1361 s	1351 m, sh	
			1353 m, sh			
1334 s	1330 s	1327 s	1322 s	1323 s	1319 s	$\nu_s(NO_2)$
1319 s, sh	1317 s					
1274 w	1265 w	1268 s	1258 m	1262 m	1261 m	ν(C–C), ν(C–F)
	1248 w	1223 w		1231 w		
1164 m	1163 w, sh	1177 m	1181 m	1180 m		ν(C–N)
	1148 m	1169 m	1167 w, sh	1167 m, sh	1161 m	
	1083 vw	1126 vw		1122 vw	1082 w	
1056 w		1056 w	1053 w	1053 w		$\nu_1(NO_3^-)$
1042 w	1045 m	1043 m	1039 w	1039 w, sh	1041 w	
		997 w				
947 m	941 w	954 m	957 w	956 w	946 w	$\rho(NH_3^+)$
922 vw	915 vw	913 w	916 w	914 vw	912 vw	
897 vw						
852 w	850 m	850 m	851 w	851 w	850 w	$\nu_2(NO_3^-)$
					841 w, sh	
823 w	823 m	825 m	823 w	826 w	825 w	
803 w	809 m				798 m	$\delta(NO_2)$
793 m	799 m	798 s	798 m	800 m	788 w, sh	
	787 w, sh					
751 w	760 w	743 vw	758 vw	760 vw	759 vw	$\nu_4(NO_3^-)$
720 w	721 w	728 w				
714 w	715 w, sh	718 w	719 w	718 w	719 w	

[a] s = strong, m = medium, w = weak, vw = very weak, sh = shoulder, br = broad.

stabilizing influence of F in the $F(NO_2)_2C-$ group promotes the proton-transfer step leading to $HNO_3(g)$. Replacement of F by NO_2 to form the $(NO_2)_3C-$ group causes C–NO_2 bond fission to predominate during thermal decomposition. The qualitative order of thermal stability of the energetic sites in these molecules is

$$F(NO_2)_2C- > -H^+\cdots NO_3^- > (NO_2)_3C-$$

These studies, coupled with previous work, suggest that the presence or absence of $NH_3(g)$ from fast thermolysis of a primary ammonium nitrate salt can be related to the O/H ratio of the parent salt.

The Solid Phase

The solid–solid phase transitions of these molecules could be interesting and complicated because of the possibility that order–disorder transitions of NO_3^- might be superimposed on phase changes stimulated by conformational changes of the cation. Illustrative of these points is the fact that NH_4NO_3 has five known phases[19] and that conformations of propylamine differ by less than 1 kcal mol^{-1}.[20] Also, the reduction in symmetry caused by substitution of F for NO_2 makes it possible to study this perturbation on the solid–solid phase transitions. We were not disappointed by the complexity of the phase transitions, especially those of FDNPAN, which prompted a careful study by DTA and IR spectroscopy. The many structural changes that take place give rise to markedly different spectra, and the transition characteristics are consistent in the IR and DTA.

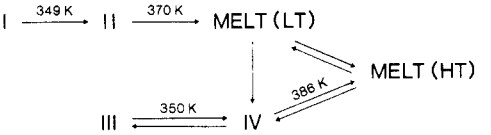

Figure 7. Solid–solid phase transition scheme above 297 K established by IR and DTA studies of FDNPAN. Two melting points exist depending on whether phase II or phase IV melts. The low-temperature melt gradually solidifies below the melting point and mostly produces solid phase IV.

The mid-IR spectra for FDNPAN and TNPAN are shown in Figure 5 along with the frequencies and tentative assignments in Tables I and II. Four solid phases of FDNPAN were discovered by heating and cooling a thin film of the sample betwen 297 K and its two melting points. The IR spectra for each phase of FDNPAN are displayed for comparison in Figure 6. Large hysteresis in the phase transitions allows the solid phases to be

(19) McLaren, A. C. *Rev. Pure Appl. Chem.* **1962**, *12*, 54.
(20) Profeta, S., Jr.; Allinger, N. L. *J. Am. Chem. Soc.* **1985**, *107*, 1907.

TABLE II: Mid-IR Frequencies (cm^{-1})[a] of TNPAN Measured at 298 K on a Thin Film of Pure Material

ν	tent. assignt	ν	tent. assignt
3120 m, sh	$\nu_{as}(NH_3^+)$, $\nu_s(NH_3^+)$	1366 vw	
3073 m, sh		1297 m	$\nu_s(NO_2)$, $\nu_3(NO_3^-)$
3035 m, sh		1162 m	ν(CN)
2979 m	$\nu_{as}(CH_2)$, $\nu_s(CH_2)$	1065 vw	$\nu_1(NO_3^-)$
2888 m		1034 vw	
2838 m, sh		996 w	$\rho(NH_3^+)$
2763 w, sh	combinations and overtones	975 w, sh	
2716 w, sh		934 vw	
2659 w		900 vw	
		875 vw	
2598 w, sh		856 w	$\nu_2(NO_3^-)$
2497 w		848 w	
1976 vw, br		837 w	
1602 s	$\nu_{as}(NO_2)$	805 m, sh	$\delta(NO_2)$
1548 w, sh	$\delta_{as}(NH_3^+)$	799 m	
1502 w	$\delta_s(NH_3^+)$	768 w	
1478 w	CH_2 scissor and wagging	735 w	$\nu_4(NO_3^-)$
1459 m			
1420 w			

[a] s = strong, m = medium, w = weak, vw = very weak, sh = shoulder, br = broad.

TABLE III: The Enthalpy Change Measured by DTA for the Phase Transitions of FDNPAN

phase transition	ΔH, kcal mol^{-1}	center temp, K
I → II	1.4	349
II → melt	9.1	370
III → IV	3.4	350
IV → melt	5.6	386

supercooled to 297 K, at least briefly. These solid phases are related by the scheme shown in Figure 7, which was confirmed by both IR spectroscopy and DTA. ΔH for each transition is given in Table III.

The IR spectra of FDNPAN(I) and FDNPAN(II) are distinctly different. It is possible that the differences in the $\nu_{as}(NO_2)$ and $\delta_{as}(NH_3^+)$ regions and $\nu_{as}(NO_3^-)$ and ν(NH)/ν(CH) arise from conformation differences of the cation in the two phases. Another possibility is that differences in the manner of hydrogen bonding affects the coupling among these modes. This problem has not been resolved because of the lack of X-ray diffraction-quality crystals. Further heating of II leads to melting which begins at 370 K and produces the spectrum for the melt phase shown in Figure 6. The IR spectrum gradually changes as this melt phase is heated to 393 K (Figure 6). The differences are especially apparent in the NO_3^- modes, suggesting that the details of ion pairing in the melt phase depend on the temperature. When the melt phase is cooled, it does not solidify at the original melting point but gradually solidifies at a lower temperature to a new phase, IV. Phases IV and III are reversibly interconvertible upon heating and cooling through 350 K. However, when phase IV is heated to the melting point, it does not melt as phase II does at 370 K, but at 386 K.

These results indicate the existence of two sets of thermally interrelated schemes of polymorphism for FDNPAN: I → II → melt and III → IV → melt. As shown in Table III, these schemes have similar sums of ΔH: 10.6 and 9.0 kcal mol^{-1}. The values of ΔS of fusion for II and IV are 25 and 14.6 eu, respectively, and are sufficiently large to demonstrate that phases II and IV of FDNPAN still possess considerable ion order.

The substitution of F by NO_2 to produce TNPAN strongly affects the behavior of the solid phase. A possible reason is the increased microsymmetry of the chain terminus afforded by such a substitution. TNPAN has only one solid–solid phase transition above 297 K which is irreversible and is centered at 331 K with ΔH = 10.4 kcal mol^{-1}. Despite the large value of ΔH, the mid-IR spectral changes are confined to slight broadening and reduced resolution of the ν(CH)/ν(NH) region. Thus, the conformation of the cation is probably unaltered by this phase transition. TNPAN begins to decompose in advance of liquefaction and, therefore, does not have a true melting point.

Overall, the replacement of an NO_2 group by F in these molecules strongly influences the behavior of the thermal decomposition and the solid phase transitions. The thermal stability of the backbone is altered to the point that the relative importance of the energetic sites in the thermal decomposition is shifted. The number and complexity of the solid–solid phase transitions of the parent salt are sharply affected by the substitution.

Acknowledgment. Samples of TNPAN and FDNPAN were generously provided by Dr. Horst G. Adolph of the Naval Surface Weapons Center. We are grateful to the Air Force Office of Scientific Research, Aerospace Sciences, for support of this work.

Registry No. VI, 108297-69-4; VII, 108297-70-7.

Theoretical Studies on the Acetylene–Vinylidene Rearrangement with a Metal Atom (Li, Be, B, Na, Mg, and Al)

Shogo Sakai* and Keiji Morokuma

Institute for Molecular Science, Myodaiji, Okazaki 444, Japan *(Received: November 6, 1986)*

Reaction mechanisms of 1,2-hydrogen migration of neutral and anionic acetylene to form corresponding vinylidenes are investigated with the ab initio Hartree–Fock method, the second- and third-order Møller–Plesset perturbation theory, and the localized molecular orbital (LMO) analysis. The LMO analysis shows that in the neutral system the migrating hydrogen behaves like a hydride (H^-) along the reaction path, while in the anion system it moves as a hydrogen atom. Reaction mechanisms of 1,2-hydrogen migration of neutral acetylene in the presence of a metal atom (Li, Be, B, Na, Mg, and Al) are also studied. The metal-catalyzed acetylene–vinylidene rearrangement can be classified based on the above two mechanisms of the metal-free reaction. In the presence of Li and Na atoms, the reaction mechanism is essentially that of the neutral acetylene, whereas with B, Be(^{3}P), Mg(^{3}P), and Al atoms, the reaction is similar to that of the acetylene anion. This difference has been related to the fact that in the latter atoms an odd electron is in a p orbital, whereas in the former no odd electron exists in a p orbital.

Introduction

The chemical reaction with a metal catalyst has been a very active area for both experimental and theoretical studies. Recently, the reaction of acetylene and ethylene with a metal atom in argon matrix[1-10] has been studied with a photoirradiation technique. In particular, the following reaction products were reported for the

(1) Kasai, P. H.; McLeod, D., Jr. *J. Am. Chem. Soc.* **1975**, *97*, 6602.

0022-3654/87/2091-3661$01.50/0